

# Leakage mechanisms in GaN-on-GaN vertical pn diodes

B. Rackauskas,<sup>1</sup> S. Dalcanele,<sup>1</sup> M. J. Uren,<sup>1</sup> T. Kachi,<sup>2</sup> and M. Kuball<sup>1</sup>

<sup>1</sup>Center for Device Thermography and Reliability (CDTR), H.H. Wills Physics Laboratory, University of Bristol, Bristol BS8 1TL, United Kingdom

<sup>2</sup>Institute of Materials and Systems for Sustainability, Nagoya University, Furo-cho, Chikusa-ku, Nagoya 464-8601, Japan

(Received 5 April 2018; accepted 21 May 2018; published online 4 June 2018)

Reverse bias leakage in bulk GaN-on-GaN pn diodes has been studied as a function of time. A peak was observed in the current transient and attributed to impurity band conduction along dislocations which is modulated by the field effect of charged decorating clusters. This model is consistent with reports of vacancy clustering around dislocations during growth. © 2018 Author(s). All article content, except where otherwise noted, is licensed under a Creative Commons Attribution (CC BY) license (<http://creativecommons.org/licenses/by/4.0/>). <https://doi.org/10.1063/1.5033436>

Gallium Nitride (GaN) is an ideal material for high power electronics due to its high electron mobility and high breakdown field, with the performance of GaN diodes exceeding the theoretical limits of SiC and demonstrating faster switching than Si diodes.<sup>1–3</sup> The development of vertical power devices allows for a higher power density. However, until recently, this technology has been limited by the availability of high quality bulk GaN with low dislocation densities.<sup>4</sup> The dislocation density in GaN-on-GaN wafers ( $\sim 10^6 \text{ cm}^{-2}$ ) is much lower than GaN grown on other substrates (e.g., silicon where dislocation density is typically  $10^9 \text{ cm}^{-2}$ ) and as reverse leakage correlates with the dislocation density, GaN-on-GaN reverse leakage currents are considerably lower than GaN-on-Si.<sup>5,6</sup> The mechanism of the reverse leakage in Si doped GaN has been an area of intensive study, with experimental work demonstrating the leakage I-V to be consistent with variable range hopping.<sup>7,8</sup> It has also been observed that the current density closely follows the dislocation density, with the compelling conclusion that dislocations are the source of the hopping states.<sup>9,10</sup> Thus it is understood that hopping takes place along the dislocation core.<sup>4</sup> This work furthers the understanding of the leakage dynamics by investigation in the time domain. The findings suggest that the leakage path is via conduction in an impurity band (IB) in the dislocation core, as recently speculated in leakage through carbon doped GaN,<sup>11,12</sup> and influenced by the field effect of charged, decorating clusters.

The GaN substrate in this study was grown by hydride vapor phase epitaxy.<sup>13,14</sup> On this, four GaN layers were grown by metal-organic chemical vapor deposition (MOCVD), starting with an interfacial  $n^+$  layer. The junction consisted of a  $5 \mu\text{m}$   $n^-$  drift region and a  $0.5 \mu\text{m}$   $p^+$  layer, doped with  $3 \times 10^{16} \text{ cm}^{-3}$  silicon and  $4 \times 10^{19} \text{ cm}^{-3}$  magnesium, respectively. Finally, a thin  $p^{++}$  layer was grown for ohmic contacting. A photoresist erosion and dry etch process was used on the p-GaN to leave a truncated conical structure with a circular pn junction, shown schematically in Fig. 1(a). The structure had an edge termination bevel angle of  $7\text{--}10^\circ$  to reduce the peak field on the surface compared to the bulk.<sup>15</sup> The device area was  $0.25 \text{ mm}^2$  with the ohmic contact metals Ti/Al on the n-GaN and Ni/Au on the p-GaN. These contact recipes

were developed for LED fabrication and deliver fully ohmic contacts. An ideality factor of 1.4 was measured for the diode, with a hard breakdown voltage of around 250 V. Current and capacitance transient measurements of 1000 s duration were performed both during and after reverse bias stress. The measurement sequence of increasing reverse bias stresses from 20 V to 100 V is shown in Fig. 1(b). The capacitance and current transients were measured during separate runs of this sequence with immediate repeat measurements giving the same result. Varying reverse bias between 0 and 100 V changed the capacitance between 30.9 pF and 7.8 pF, corresponding to a depletion width increasing from  $0.6 \mu\text{m}$  to  $2.5 \mu\text{m}$ .

The capacitance and current transients during stress, shown in Fig. 2, exhibited a small relaxation which lasted for  $>1000 \text{ s}$  with a feature whose position in time was voltage dependent. For the capacitance transients, this feature was a small plateau, whereas in the current transients, this was a

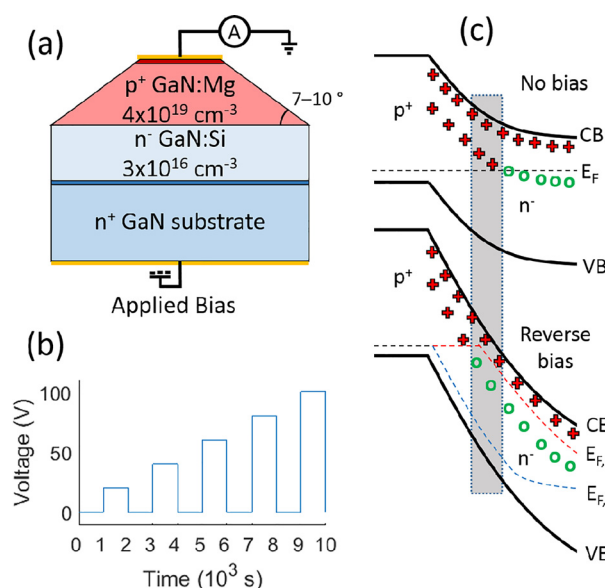


FIG. 1. (a) The device cross-section and wiring diagram. (b) The sequence of the transient measurements. Between each 1000 s stress was a filling/recovery phase of 1000 s. (c) Sketches of the equilibrium band structures of a pn junction, containing both a shallow and deep donor, at the indicated bias conditions. The shaded area indicates the few nanometres near the junction in which deep traps (donors in this example) can change state.

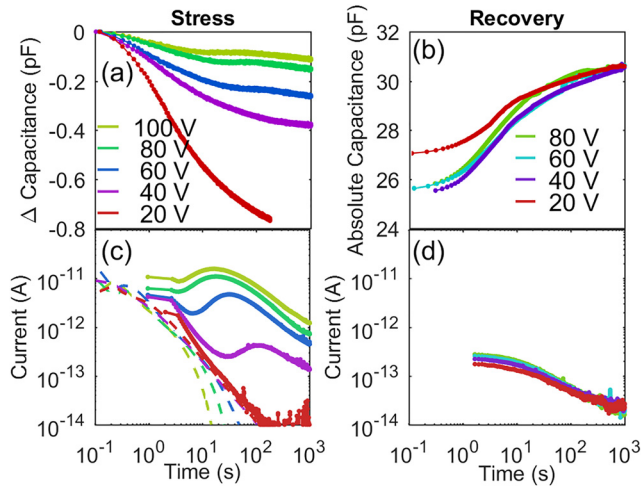


FIG. 2. Transients of (a) capacitance and (c) current, during reverse bias stress. Increasing reverse bias caused a smaller capacitance transient. The diode area was  $0.25 \text{ mm}^2$  and the static capacitance was  $\sim 30.9 \text{ pF}$ . The dashed lines in (c) are the calculated displacement current from the capacitance gradient in (a). Parts (b) and (d) show the recovery after the indicated reverse bias stress. During the recovery, both terminals were at  $0 \text{ V}$ . The sign of the current in (d) is opposite to that in (c).

peak, visible for bias  $> 20 \text{ V}$ . The total charge involved in the capacitance transients ( $V \cdot \Delta C$ ) was approximately constant for all stresses at  $(3.8 \pm 0.4) \times 10^{10} \text{ cm}^{-2}$ . Recovering after the stress was removed, the transients extended over similar time scales. The observed recovery current transient had the opposite sign to that seen during the stress. The charge during the recovery current transient (calculated by integrating the current over time) was also approximately constant after all stress voltages but about five times larger in magnitude  $(2.31 \pm 0.04) \times 10^{11} \text{ cm}^{-2}$ . Across the sample, some variability was seen in the amplitude of these features, with the data shown here being one of the most distinct cases. Interestingly, the transients showed no strong trend with increasing temperature where behaviour was largely the same in the tested  $30\text{--}120^\circ\text{C}$  range. The current transients during a reverse bias stress of 100 and  $20 \text{ V}$  are shown in Fig. 3 at various temperatures.

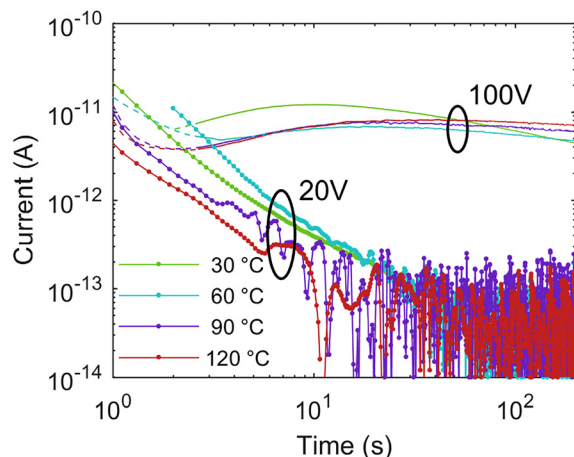


FIG. 3. Current transients during a reverse bias stress of  $20 \text{ V}$  and  $100 \text{ V}$  over a temperature range of  $30\text{--}120^\circ\text{C}$ . The transients are only weakly temperature dependent with no trend emerging.

The decreasing capacitance during stress implies the depletion region was expanding, either by  $1\text{--}3\%$  in the n-GaN or by  $40\text{--}110\%$  in the p-GaN (assuming  $1\%$  activation<sup>16</sup>). It has not been possible to distinguish which one of those is occurring and both are plausible. Although there have been previous reports of current transient peaks being observed in reverse biased pn junctions, these have been in conjunction with a shrinking depletion region and were the result of the increased emission rate of deep states due to Poole-Frenkel emission as the field increased.<sup>17</sup> Whereas here, the depletion region was expanding so this model cannot explain the transient features. Mechanisms based on the summation of multiple trap states with different time constants cannot explain the behaviour. Surface leakage was disregarded as a mechanism since there was no difference in the transient current when illuminating the bulk or surface of the junction with below bandgap light. If surface leakage were the cause of the transient, illumination of the bulk would have no effect whilst surface illumination would increase the current by lowering the barrier to hopping. This was not seen, therefore, to explain the shape of these transients, a different model is required.

Regardless of which side the expansion occurs, it must be driven by a reduction of the net trap charge density i.e., a reduction of the net positive (negative) trap charge on the n-(p)-side. Considering here only the case of n-side expansion (though the analog can be applied equally on the p-side), this means during the stress ionised deep donors are neutralised, or neutral deep acceptors are ionised. Considering a simple pn junction, the only region where this can happen is limited to a few nanometres on the n-side of the pn junction as depicted in Fig. 1(c). In this sketch, the quasi-Fermi levels split as carriers are swept out of the depletion region, and as a result, the quasi-Fermi level for electrons and holes ( $E_{F,n}$  and  $E_{F,p}$ ) move down and up, respectively. Within a few nanometres of the junction, the quasi-Fermi level for holes can move above a donor trap level during reverse bias to produce the observed reducing capacitance transient.

Our model breaks the current transient down into two components. The first is related to emission which must be present to cause the capacitance transient. Any capacitance transient is caused by a changing charge density which in this case on the n-side is due to the capture of electrons or emission of holes, and will give rise to a transitory displacement current which is related to the capacitance by

$$I(t) = V \frac{dC(t)}{dt} + C(t) \frac{dV}{dt}. \quad (1)$$

Since in this measurement  $V$  is constant, the second term is zero and the displacement current is directly proportional to the rate of capacitance change. This current, predicted from the capacitance transients with Eq. (1), is compared with the measured current transients in Fig. 2(c) as dashed lines. In the initial phase of the transient at short times, and which is best seen in the  $20 \text{ V}$  and  $40 \text{ V}$  transients, the measured current transient is in reasonable agreement with that predicted from the capacitance transient. This implies that this portion of the current transient is primarily a direct result of the capture of electrons or the emission of holes in the depletion region. However, it cannot explain the peak seen in Fig. 2(c).

At higher stress voltages, or longer times, an increase in the current is observed above that associated with the change of the charge state of traps, reaching a peak and then followed by a slow decrease. Hence, this must be associated with the turn-on and subsequent relaxation of a leakage path between the contacts. Here, we suggest that this is attributed to the “turning on” of dislocation leakage. We assume that the rate limiting step for transport in the peak is along the dislocation, and that contact between the dislocation and the  $n+$  and  $p++$  contacts is lower resistance, perhaps involving a tunnelling mechanism. One possible model is based on the observation that vacancies in GaN diffuse through the crystal during growth and gather at extended defects.<sup>18</sup> It is proposed that the changing occupancy of the trap states clustered around the dislocation drives the capacitance change, as well as gates the dislocation and modulates its conductivity. Presuming variable range hopping (VRH) as the conduction mechanism along the dislocation core,<sup>4,19</sup> the hopping probability depends on the density of trap states around the Fermi level.<sup>20,21</sup> The field effect from the clusters of traps can change the occupancy of the dislocation core states, and if they are in a defect band, then maximum conductivity will arise when it is half occupied. Therefore, movement of the Fermi level through an impurity band [by (dis)charging the clustered states] would result in a peak in the conductivity of the dislocation core as the occupancy of the band changes from empty to full (a 1D analog of the findings of Fowler and Hartstein<sup>22</sup>). Here, we propose that the (dis)charging of the clustered trap states (1) changes the net charge density and generates the capacitance transient, (2) gives rise to a transitory displacement current, and (3) moves the Fermi level through an impurity band thus creating a peak in the conductivity along the dislocation core.

A qualitative example of how clustered states can cause a transient shift in the Fermi level is shown in Fig. 4 and this is related to the observed current transient behaviour in Fig. 5. This example uses deep donors in n-GaN, but the

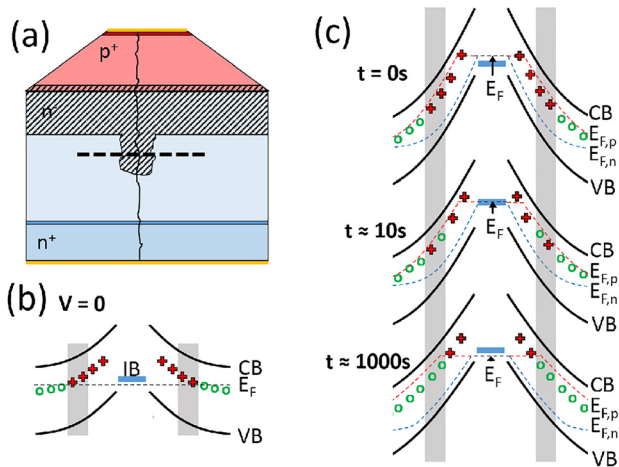


FIG. 4. (a) A schematic cross-section of the pn diode with one dislocation, the dashed line is the outline for (b) and (c), and the shaded area represents depletion. The band diagram of the dislocation showing only a deep donor level is represented, (b) before applied bias, and (c) during the transient resulting from stress. In (c), the Fermi level at the dislocation is determined by the occupancy of the surrounding states. The shaded area in the dislocation core represents an impurity band (IB). This example is assuming deep donor states are surrounding the dislocation.

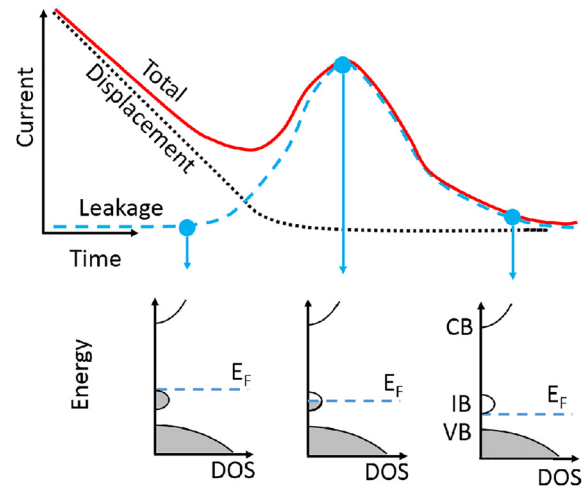


FIG. 5. The mechanism by which an impurity band can give rise to a transient current peak. The transient current is shown decomposed into the displacement and leakage current components with energy vs density of states (DOS) diagrams before, during, and after the leakage current peak. As the Fermi level is driven through the impurity band (like by a field effect as in Fig. 4), the density of states increases from zero and goes through a maximum.

same effect can be applied with any deep trap in n-type or p-type GaN. Threading dislocations in n-GaN have been directly observed to be negatively charged with the potential in the core reduced by up to 2.5 V within 10 nm.<sup>23–25</sup> Conversely, dislocations in p-GaN are positively charged.<sup>23,26</sup> This makes the dislocation in n-GaN slightly p-type resulting in the equilibrium band-structures shown in Fig. 4(b), here we assume the core contains an impurity band and is surrounded by ionised deep donor clusters. Under the assumption that the p-GaN layer and the dislocation core are electrically in contact, putting the diode in reverse bias will also put the dislocation core in reverse bias within the n-type layer. This will cause the deep donor states to discharge and become neutral over  $\sim 1000$  s [Fig. 4(c)], presumably by hole tunnelling to the dislocation core (a temperature independent process<sup>27</sup>). The result is a reducing net depletion charge, reducing effective doping density (bulk capacitance decreases) and a decreasing Fermi-level in the core which, supposing an impurity band in that region, would lead to a peak in conductivity demonstrated in Fig. 5. Figure 4(a) shows a cross-section of the diode with a single dislocation, the depletion region extends further into the drift region around the dislocation as the charge density is locally reduced.

This model results in the transient process being temperature independent as seen in Fig. 3. The recovery transients in Figs. 2(b) and 2(d) are also consistent with this model; the capacitance increases due to increasing net positive charge density as the clustered states return to their equilibrium charge state. The sign of the recovery current transient is opposite to that during the stress stage and shows no peak. Despite the Fermi level passing back through the impurity band and modulating the dislocation conductivity, it would produce no current since there is no applied field. Instead, the recovery current transient is attributed only to the displacement current from the recovering capacitance transient. In this case, the measured current cannot be compared with an expected displacement current as the potential distribution through the device [required for Eq. (1)] is not known.



Current and capacitance transients have been used as a method to study the leakage mechanisms in GaN-on-GaN vertical pn diodes. The transients showed surprising features which are not possible to explain using conventional trapping models. It is instead suggested that this is the first direct evidence of impurity band conduction along dislocations with the conductivity influenced by the field effect of decorating clusters. One possibility is these are clusters of vacancies which migrate towards the dislocation during growth. Off state leakage is a critical parameter for power diodes and it is essential to understand the cause of transient behaviour if it is to be improved.

B. Rackauskas acknowledges funding from the UK EPSRC. Supporting data available at <https://doi.org/10.5523/bris.luxzbqest814t2196741nyw0ea>.

- <sup>1</sup>I. C. Kizilyalli, A. P. Edwards, H. Nie, D. Disney, and D. Bour, *IEEE Trans. Electron Devices* **60**, 3067 (2013).
- <sup>2</sup>D. Disney, H. Nie, A. Edwards, D. Bour, H. Shah, and I. C. Kizilyalli, in *2013 25th International Symposium on Power Semiconductor Devices IC's* (IEEE, 2013), pp. 59–62.
- <sup>3</sup>K. Nomoto, B. Song, Z. Hu, M. Zhu, M. Qi, N. Kaneda, T. Mishima, T. Nakamura, D. Jena, and H. G. Xing, *IEEE Electron Device Lett.* **37**, 161 (2016).
- <sup>4</sup>Y. Zhang, H.-Y. Wong, M. Sun, S. Joglekar, L. Yu, N. A. Braga, R. V. Mickevicius, and T. Palacios, in *2015 IEEE International Electron Devices Meeting* (IEEE, 2015), p. 35.1.1–35.1.4.
- <sup>5</sup>I. C. Kizilyalli, T. Prunty, and O. Aktas, *IEEE Electron Device Lett.* **36**, 1073 (2015).
- <sup>6</sup>Y. Zhang, M. Sun, H.-Y. Wong, Y. Lin, P. Srivastava, C. Hatem, M. Azize, D. Piedra, L. Yu, T. Sumitomo, N. A. de Braga, R. V. Mickevicius, and T. Palacios, *IEEE Trans. Electron Devices* **62**, 2155 (2015).
- <sup>7</sup>D. V. Kuksenkov, H. Temkin, A. Osinsky, R. Gaska, and M. A. Khan, *Appl. Phys. Lett.* **72**, 1365 (1998).
- <sup>8</sup>Q. Shan, D. S. Meyaard, Q. Dai, J. Cho, E. Fred Schubert, J. Kon Son, and C. Sone, *Appl. Phys. Lett.* **99**, 253506 (2011).
- <sup>9</sup>D. S. Li, H. Chen, H. B. Yu, H. Q. Jia, Q. Huang, and J. M. Zhou, *J. Appl. Phys.* **96**, 1111 (2004).
- <sup>10</sup>X. Cao, J. Teetsov, F. Shahedipour-Sandvik, and S. Arthur, *J. Cryst. Growth* **264**, 172 (2004).
- <sup>11</sup>C. Koller, G. Pobegen, C. Ostermaier, M. Huber, and D. Pogany, *Appl. Phys. Lett.* **111**, 32106 (2017).
- <sup>12</sup>C. Koller, G. Pobegen, C. Ostermaier, and D. Pogany, in *2017 IEEE International Electron Devices Meeting* (IEEE, 2017), p. 33.4.1–33.4.4.
- <sup>13</sup>K. Fujito, S. Kubo, H. Nagaoka, T. Mochizuki, H. Namita, and S. Nagao, *J. Cryst. Growth* **311**, 3011 (2009).
- <sup>14</sup>A. Usui, H. Sunakawa, A. Sakai, and A. A. Yamaguchi, *Jpn. J. Appl. Phys.* **36**, L899 (1997).
- <sup>15</sup>S. M. Sze, *Physics of Semiconductor Devices* (John Wiley & Sons, 1981).
- <sup>16</sup>W. Götz, N. M. Johnson, J. Walker, D. P. Bour, H. Amano, and I. Akasaki, *Appl. Phys. Lett.* **67**, 2666 (1995).
- <sup>17</sup>E. Rosencher, V. Mosser, and G. Vincent, *Phys. Rev. B* **29**, 1135 (1984).
- <sup>18</sup>K. Horibuchi, S. Yamaguchi, Y. Kimoto, K. Nishikawa, and T. Kachi, *Semicond. Sci. Technol.* **31**, 34002 (2016).
- <sup>19</sup>V. Moroz, H. Y. Wong, M. Choi, N. Braga, R. V. Mickevicius, Y. Zhang, and T. Palacios, *ECS J. Solid State Sci. Technol.* **5**, P3142 (2016).
- <sup>20</sup>R. M. HILL, *Nature* **204**, 35 (1964).
- <sup>21</sup>R. M. Hill, *Phys. Status Solidi* **34**, 601 (1976).
- <sup>22</sup>A. B. Fowler and A. Hartstein, *Philos. Mag. B* **42**, 949 (1980).
- <sup>23</sup>D. Cherns, C. G. Jiao, H. Mokhtari, J. Cai, and F. A. Ponce, *Phys. Status Solidi* **234**, 924 (2002).
- <sup>24</sup>C. Jiao, *J. Electron Microsc. (Tokyo)*, **51**, 105 (2002).
- <sup>25</sup>D. Cherns and C. G. Jiao, *Phys. Rev. Lett.* **87**, 205504 (2001).
- <sup>26</sup>A. F. Wright and U. Grossner, *Appl. Phys. Lett.* **73**, 2751 (1998).
- <sup>27</sup>L. Esaki, *Phys. Rev.* **109**, 603 (1958).